Rate Coefficients for the Reactions of OH with $CF_3CH_2CH_3$ (HFC-263fb), CF_3CHFCH_2F (HFC-245eb), and $CHF_2CHFCHF_2$ (HFC-245ea) between 238 and 375 K†

B. Rajakumar,[||,‡] R. W. Portmann,[||] James B. Burkholder,[||] and A. R. Ravishankara*[,||,§]

National Oceanic and Atmospheric Administration, Earth System Research Laboratory, 325 Broadway, Boulder, Colorado 80305, and The Cooperative Institute for Research in Environmental Sciences, University of Colorado, Boulder, Colorado 80309

Received: October 30, 2005; In Final Form: December 25, 2005

Rate coefficients for reaction of the hydroxyl radical (OH) with three hydrofluorocarbons (HFCs) $CF_3CH_2CH_3$, HFC-263fb, (k_1); CF_3CHFCH_2F, HFC-245eb, (k_2); and $CHF_2CHFCHF_2$, HFC-245ea, (k_3); which are suggested as potential substitutes to chlorofluorocarbons (CFCs), were measured using pulsed laser photolysis−laser-induced fluorescence (PLP−LIF) between 235 and 375 K. The Arrhenius expressions obtained are $k_1(T) = (4.36 \pm 0.72) \times 10^{-12} \exp[-(1290 \pm 40)/T]$ cm^3 molecule^{-1} s^{-1}; $k_2(T) = (1.23 \pm 0.18) \times 10^{-12} \exp[-(1250 \pm 40)/T]$ cm^3 molecule^{-1} s^{-1}; $k_3(T) = (1.91 \pm 0.42) \times 10^{-12} \exp[-(1375 \pm 100)/T]$ cm^3 molecule^{-1} s^{-1}. The quoted uncertainties are 95% confidence limits and include estimated systematic errors. The present results are discussed and compared with rate coefficients available in the literature. Our results are also compared with those calculated using structure activity relationships (SAR) for fluorinated compounds. The IR absorption cross-sections at room temperature for these compounds were measured over the range of 500 to 4000 cm^{-1}. The global warming potentials (GWPs) of $CF_3CH_2CH_3$(HFC-263fb), CF_3CHFCH_2F(HFC-245eb), and $CHF_2CHFCHF_2$(HFC-245ea) were calculated to be 234, 962, and 723 for a 20-year horizon; 70, 286, and 215 for a 100-year horizon; and 22, 89, and 68 for a 500-year horizon; and the atmospheric lifetimes of these compounds are 0.8, 2.5, and 2.6 years, respectively. It is concluded that these compounds are acceptable substitutes for CFCs in terms of their impact on Earth's climate.

Introduction

Chlorofluorocarbons (CFCs) have been shown to be detrimental to Earth's stratospheric ozone layer.[1] Therefore, the Montreal protocol[2] and its amendments have been accepted internationally. This decision has prompted industry to look for alternatives to CFCs in various applications.[1] Partially fluorinated hydrocarbons (HFCs) are among the leading environmentally acceptable CFC alternatives from the point of view of ozone depletion. However, HFCs absorb strongly in the IR region of the Earth's outgoing radiation. Therefore, for HFCs to be environmentally acceptable, their contribution to the greenhouse effect needs to be small. Quantification of the possible role of HFCs as greenhouse gases requires accurate information on their lifetimes and IR absorption cross-sections, which are key parameters in determining their global warming potentials (GWPs), a relative index of the greenhouse potential of a gas.

Because of the presence of one or more C−H bonds, HFCs react with tropospheric hydroxyl radicals, resulting in atmospheric lifetimes shorter than those of CFCs. Yet, their reactivity with OH is sufficiently slow that their atmospheric lifetimes can be years.

The three HFCs studied here, $CF_3CH_2CH_3$ (HFC-263fb), CF_3CHFCH_2F (HFC-245eb), and $CHF_2CHFCHF_2$ (HFC-245ea), are among a class of compounds that are potential substitutes to CFCs.[1] The rate coefficients for the reaction of these compounds with OH, to the best of our knowledge, have only been reported by Nelson et al.,[3] and only at room temperature. A theoretical investigation by Percival et al.[4] has reported the temperature dependence of the title reactions. The lack of experimentally determined rate coefficients at atmospheric temperatures has led us to the present investigation.

In this paper, we present the rate coefficient for the reaction of OH radicals with $CF_3CH_2CH_3$, CF_3CHFCH_2F and $CHF_2CHFCHF_2$ between 238 and 375 K.

$$OH + CF_3CH_2CH_3 \xrightarrow{k_1} \text{products} \quad (1)$$

$$OH + CF_3CHFCH_2F \xrightarrow{k_2} \text{products} \quad (2)$$

$$OH + CHF_2CHFCHF_2 \xrightarrow{k_3} \text{products} \quad (3)$$

In addition, we report the IR absorption cross-sections, atmospheric lifetimes and GWPs for these compounds.

Experimental Section

In this work, the rate coefficients for the title reactions, $k_1(T)$, $k_2(T)$, and $k_3(T)$ were determined in the temperature range 238−375 K. Also, infrared absorption cross-sections for $CF_3CH_2CH_3$, CF_3CHFCH_2F, and $CHF_2CHFCHF_2$ were determined at 298 K. We have described the apparatus, data acquisition methods, and data analysis procedures for measuring rate coefficients for reactions with OH[5] in previous publications.

† Part of the special issue "David M. Golden Festschrift".

* Correspondence to A. R. Ravishankara (A. R.Ravishankara@noaa.gov); NOAA, Earth System Research Laboratory, Chemical Sciences Division, R/CSD 2, 325 Broadway, Boulder, CO 80305.

|| National Oceanic and Atmospheric Administration.

‡ CIRES, University of Colorado.

§ Also affiliated with the Department of Chemistry and Biochemistry, University of Colorado, Boulder, CO 80309.

10.1021/jp056248y CCC: $33.50
Published on Web 03/04/2006

Therefore, we only briefly describe here the essentials needed to understand the present investigation.

Rate Coefficient Measurements. The rate coefficients k_1-k_3 were determined under pseudo-first-order conditions in OH concentration using pulsed laser photolysis (PLP) production of OH and its laser-induced fluorescence (LIF) detection. The LIF reactor consisted of a 15-cm-long jacketed Pyrex cell with an internal volume of ~200 cm^3. Orthogonal ports on the reactor were used to propagate the laser beams. The photomultiplier tube (PMT) detector was mounted on a port orthogonal to the laser beams. The LIF reactor temperature was regulated to ±1 K by circulating heated/cooled silicon oil through its jacket. The gas mixture entering the reactor attained the temperature of the reactor before reaching the reaction zone, defined by the intersection of the photolysis beam and probe laser beam. The temperature of the gases in the reaction zone was directly measured with a calibrated thermocouple inserted into the gas flow. The thermocouple was withdrawn from the detection region while measuring the OH temporal profiles. Pressures in the LIF reactor were measured with a 10, 100, or 1000 Torr capacitance manometer.

Rate coefficients were measured at total pressures in the range of 50 to 60 Torr (He) with linear gas flow velocities in the LIF reactor of 10 to 20 cm s^{-1}. This flow provided a fresh gas mixture for each photolysis laser pulse (10 Hz).

OH radicals were produced by 248 nm excimer (KrF) laser photolysis of H_2O_2

$$H_2O_2 + h\nu \rightarrow OH + OH \qquad (4)$$

where the quantum yield for OH production in reaction 4 is 2.

OH radicals were excited in the $A^2\Sigma^+ \leftarrow X^2\Pi$ band (282 nm) using the frequency-doubled output of a pulsed Nd:YAG pumped dye laser. The laser-induced fluorescence was detected by a PMT after it passed through a band-pass filter (peak transmission at 310 nm with a band-pass of ±20 nm, fwhm). The PMT signal was averaged at various reaction times, ranging from 10 μs to 50 ms, with a gated charge integrator and recorded for subsequent analysis.

The initial OH radical concentration, $[OH]_0$, was estimated from the measured laser fluence (varied over the range 1.0−6.8 mJ cm^{-2} $pulse^{-1}$), the absorption cross-section of the precursor at the photolysis wavelength, its OH quantum yield, and the precursor concentration. $[OH]_0$ values in the range 1.2×10^{11} to 7.5×10^{11} molecule cm^{-3} were used over the course of the kinetic measurements.

The concentration of H_2O_2 in the LIF reactor was estimated from the first-order rate coefficient for loss of OH measured in the absence of the reactant and attributed to the reaction of OH with H_2O_2

$$OH + H_2O_2 \rightarrow HO_2 + H_2O \qquad (5)$$

where $k_5(T) = 2.9 \times 10^{-12} \exp(-160/T)$ cm^3 $molecule^{-1}$ s^{-1}.[6] The concentration of H_2O_2 in the LIF reactor was varied between 1.6×10^{13} and 1.2×10^{14} molecule cm^{-3} over the course of the kinetic measurements but was maintained constant during each individual rate coefficient determination. The ozone concentration in the LIF reactor, typically 1×10^{12} molecule cm^{-3}, was determined from measured flow rates and pressures.

The concentrations of the HFC reactants were determined by two independent methods. It should be noted that the concentrations of the reactant in the reactor were not directly measured. The reactant concentration prior to entering the reactor was determined from the flow rate measured using calibrated electronic mass flow meters. Flow meters were calibrated independently for each reactant. The reactant concentration in the gas flow was also measured by infrared absorption at 298 K as described below. The reactant concentration in the reactor was corrected for the differences in temperature and pressure and for dilution. The concentrations of $CF_3CH_2CH_2$, CF_3CHFCH_2F, and $CHF_2CHFCHF_2$ in the reactor were varied in the ranges $(2.8-44) \times 10^{14}$, $(2.2-54) \times 10^{14}$, and $(2.3-66) \times 10^{14}$ molecule cm^{-3}, respectively. The concentration determined using flow rates agreed with that from infrared absorption measurements to within ±5% under all experimental conditions.

Infrared Absorption Cross-Section Measurements. Infrared (IR) absorption cross-sections of the HFCs were measured using a Fourier transform infrared spectrometer (FTIR) equipped with a 15-cm-long, 2.5-cm-diameter Pyrex absorption cell with KBr windows. An incandescent light source, KBr beam splitter, and liquid N_2 cooled HgCdTe (MCT) detector were used. Spectra were recorded at a spectral resolution of 1 cm^{-1} over the range 500 to 4000 cm^{-1} with 100 coadded scans. The IR cross-sections were measured by filling the absorption cell with 1−3 Torr of the compound measured using a 10 Torr capacitance manometer. A minimum of 6 concentrations were used for each compound. The peak absorbance for each band varied linearly with concentration, i.e., obeyed Beer−Lambert's law. Peak absorption cross-sections were obtained using linear least-squares fits of absorbance versus concentration. The absorption spectra over the entire wavelength region were converted to cross-sections using the cross-sections derived at the peaks. The cross-sections derived from different peak cross-sections agreed within 5%. Spectrum measurements were also made with the absorption cell pressurized with 100 Torr of N_2 to investigate the broadening of the HFC bands; the bands were not broadened at this pressure. Therefore, the IR cross-sections obtained using the samples alone are applicable under atmospheric pressures.

Materials. He (99.999%) was used as supplied as the buffer gas in all the kinetic measurements. Nitrogen (>99.99%) was used as supplied in the measurement of IR absorption cross-sections. Concentrated hydrogen peroxide (>95%, by mole fraction, as determined by titration with a standard solution of $KMnO_4$) was prepared by bubbling N_2 for several days through a H_2O_2 sample which was initially ~60% by mole fraction. A small flow of He, approximately 1% of the total gas flowing through the reactor, was passed through a bubbler containing the >95% pure liquid H_2O_2. This mixture from the bubbler was added to the main gas flow before entering the LIF reactor. During low-temperature kinetic measurements, the H_2O_2 reservoir was maintained at a temperature lower than that of the LIF reactor to avoid possible condensation of H_2O_2 in the cold reactor. Ozone was prepared by passing O_2 through a commercial ozonizer and stored on a silica gel at 195 K. A dilute mixture of ozone in He was prepared in a darkened Pyrex bulb from this sample.

Impurities in Excess Reactant. The rate coefficients for reactions 1−3 are relatively small, $<2 \times 10^{-13}$ cm^3 $molecule^{-1}$ s^{-1}, and hence, reactive impurities can lead to systematic errors in the measured values. Unsaturated hydrocarbon impurities, which can react with OH with rate coefficients of up to 3 orders of magnitude faster than the HFCs, are therefore of concern. The HFC samples were analyzed by gas chromatography−mass spectroscopy (GCMS) using a capillary GS−Al column. No measurable impurities were observed in the $CF_3CH_2CH_3$ sample. The CF_3CHFCH_2F sample was found to have trace amounts, <100 ppmv, of $CF_3CHFCHF_2$, $CF_3CH_2CH_2CF_3$, and

CF_3CHFCH_3. The $CHF_2CHFCHF_2$ sample was found to have $CF_3CH{=}CF_2$. We have estimated the $CF_3CH{=}CF_2$ abundance to be ~50 ppmv by assuming a mass detector response similar to that of $CH_3CH{=}CH_2$. This level of impurity would increase the observed k_3 value by ~5% at 298 K and ~20% at 238 K. We have also checked for the presence of unsaturated hydrocarbons using a purification test, which consisted of passing the reactant through a column containing sulfuric acid (20 wt % deposited on Chromosorb WHP). Sulfuric acid would remove unsaturated compounds from the sample. For the rate coefficient measurements, the reactant samples were introduced into the gas flow after passing through the calibrated mass flow meters. The small impurity levels of the samples do not contribute significant error to the measured IR absorption cross-sections.

Results and Discussions

All rate coefficients were measured under pseudo-first-order conditions in OH with [reactant] ≥ 1000[OH]$_0$. Under these conditions, the OH temporal profiles followed the pseudo-first-order rate law

$$\ln[\mathrm{OH}]_t = \ln[\mathrm{OH}]_0 - k't \tag{6a}$$

or

$$\ln(S_t) = \ln(S_0) - k't \tag{6b}$$

where k' (= k_1[reactant] + k_d') is the pseudo-first-order rate coefficient for the reaction of OH with the reactant, and S_t and S_0 are the LIF signals from OH at time t and time zero, respectively. k_d' is the pseudo-first-order rate coefficient for loss of OH in the absence of the reactant. k_d' is attributed to the sum of the first-order rate coefficients for diffusion of OH out of the detection zone and its reaction with the photochemical precursor and possible impurities in the bath gas. Typical measured values of k_d' were in the range 80−300 s^{-1}.

Values of k' were obtained from an unweighted linear least-squares fit of the measured values of S_t as a function of reaction time to eq 6b. In all cases, the measured OH profiles were exponential, confirming that the loss rates of OH were pseudo-first order in [OH]. At each temperature, $k_1(T)$ was obtained from a linear least-squares fit of the measured values of k' obtained at various concentrations of the reactant to the equation: $k' = k_1$[reactant] + k_d. Figure 1 shows $k_1(T)$, $k_2(T)$, and $k_3(T)$ values that were obtained from data collected at the temperature extremes of the current study. Under all conditions, k' varied linearly with the concentration of HFC, and the linear least-squares fits to the data were very precise. Tables 1−3 give a summary of the experimental conditions used in the determination of k_1−k_3 along with the obtained rate coefficients.

Uncertainties in the Measured Values of *k*′. We estimate the systematic uncertainties in the measured parameters to be relatively small: ±1% in total pressure, ±2% in flow rate, and <1% in temperature. The precision of the first-order rate coefficient, k', was on the order of a few percent, and the uncertainty in the slopes of the k' versus the concentration of HFC were also small. The largest source of uncertainty in the present study lies in the determination of reactant concentration in the LIF reactor. The concentration of the reactant was determined using two independent methods: (a) using flow rates (measured using calibrated mass flow meters) and pressure and (b) via direct IR absorption. The reactant concentration determined by the two independent methods agreed to better than 5% under all experimental conditions. On this basis, we estimate the systematic uncertainty in the reactant concentration in the LIF reactor to be ±8% at the 95% confidence level.

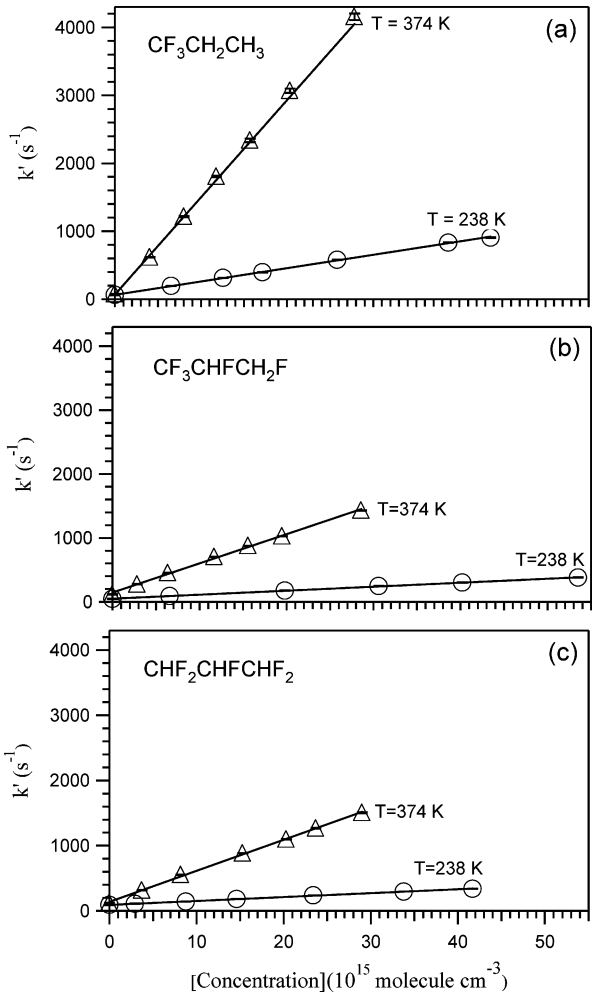

Figure 1. Plots of the measured first-order rate coefficient, k', against the concentration of the reactants (a) $CF_3CH_2CH_3$, (b) CF_3CHFCH_2F, and (c) $CHF_2CHFCHF_2$ at 238 K (circles) and 373 K (triangles). The lines are the linear least-squares fit of the data to eq 6b. The figure shows that k_1 is larger than k_2 while k_2 and k_3 are nearly equal.

Another possible source of systematic error in the measured values of $k(T)$ is the contributions from reactions of OH with impurities in the reactants. As mentioned earlier, $CF_3CH_2CH_3$ did not have any measurable impurities. Hence, the contribution due to the impurities in the measurement of k_1 is negligible. This conclusion was further checked by measuring k_1 after passing the sample through a column containing sulfuric acid (20 wt % deposited on Chromosorb WHP). This column selectively removed olefins and, hence, the reactive impurities. The measured value of k_1 was the same (see Table 1) at the lowest temperature of the study, where the impurities are expected to contribute the most. Therefore, we are confident that the measured value of k_1 is not influenced by reactive impurities. In the case of CF_3CHFCH_2F, trace amounts of $CF_3CHFCHF_2$, $CF_3CH_2CH_2CF_3$, and CF_3CHFCH_3 were observed in the sample. However, the rate coefficients for the reactions of OH with these impurities are roughly the same as that with CF_3CHFCH_2F; therefore, their presence did not

TABLE 1: Summary of the Experimental Conditions and Rate Coefficients for the Reaction OH + $CF_3CH_2CH_3$ (HFC-263fb)

temperature K	pressure Torr	flow rate cm s^{-1}	$[H_2O_2]$,10^{13} molecule cm^{-3}	$[OH]_0$, 10^{11} molecule cm^{-3}	laser fluence mJ cm^{-2} $pulse^{-1}$	$[CF_3CH_2CH_3]$, 10^{14} molecule cm^{-3}	k_1, 10^{-14} cm^3 $molecule^{-1}$ s^{-1}
238	50	6.0	3.19	2.75	4.8	6.53−43.6	1.96 ± 0.04[b]
238[a]	50	6.2	6.45	5.57	4.8	6.62−41.3	1.97 ± 0.02
256	50	6.5	3.68	3.35	5.1	8.91−35.0	2.71 ± 0.06
274	52	7.3	3.05	2.78	5.1	5.18−27.0	3.96 ± 0.08
297	52	7.3	3.18	2.32	4.1	3.97−32.9	5.42 ± 0.04
297	52	17.6	3.35	3.35	5.6	2.80−16.6	5.55 ± 0.14
297	210	6.3	1.60	1.60	5.6	4.83−30.4	5.54 ± 0.04
297	52	7.3	5.25	1.19	1.3	9.46−41.8	5.48 ± 0.08
323	50	8.2	3.58	3.25	5.1	3.68−27.5	8.03 ± 0.12
348	50	8.7	3.77	3.42	5.1	5.28−20.1	10.7 ± 0.10
373	50	9.3	3.89	3.54	5.1	4.05−27.8	14.3 ± 0.10

[a] Experiments carried out by passing the sample through a purification column containing sulfuric acid (20 wt %) deposited on Chromosorb WHP. [b] The quoted uncertainties are the 2σ (95% confidence limit) precision from the least-squares fit of the measured k' data to eq 6.

TABLE 2: Summary of the Experimental Conditions and Rate Coefficients for the Reaction OH + CF_3CHFCH_2F (HFC-245eb)

temperature K	pressure Torr	flow rate cm s^{-1}	$[H_2O_2]$, 10^{13} molecule cm^{-3}	$[OH]_0$, 10^{11} molecule cm^{-3}	laser fluence mJ cm^{-2} $pulse^{-1}$	$[CF_3CHFCH_2F]$, 10^{14} molecule cm^{-3}	k_2, 10^{-14} molecule cm^{-3} s^{-1}
238	50	6.2	2.35	2.14	5.1	6.57−53.5	0.63 ± 0.01[b]
238[a]	52	6.3	5.2	4.26	4.6	3.90−51.8	0.63 ± 0.01
254	50	6.8	2.50	2.28	5.1	5.64−42.6	0.94 ± 0.01
272	51	7.0	4.4	3.20	4.1	5.40−42.7	1.22 ± 0.02
297	51	7.4	2.83	2.7	5.3	10.2−40.4	1.81 ± 0.04
297	49	18.7	4.22	4.03	5.3	2.91−13.5	1.79 ± 0.08
297	210	6.4	1.52	1.38	5.1	4.69−36.6	1.79 ± 0.06
297	50	7.5	11.7	3.72	1.8	3.47−27.3	1.80 ± 0.08
324	51	8.3	4.33	3.35	4.3	5.75−35.3	2.50 ± 0.06
348	50	8.5	5.0	3.87	4.3	2.15−30.1	3.43 ± 0.08
349	50	8.8	7.05	5.45	4.3	5.15−30.3	3.39 ± 0.12
374	50	9.6	5.8	4.49	4.3	2.86−28.6	4.58 ± 0.08

[a] Experiments carried out by passing the sample through a purification column containing sulfuric acid (20 wt %) deposited on Chromosorb WHP. [b] The quoted uncertainties are the 2σ (95% confidence limit) precision from the least-squares fit of the measured k' data to eq 6.

TABLE 3: Summary of the Experimental Conditions and Rate Coefficients for the Reaction OH + $CHF_2CHFCHF_2$ (HFC-245ea)

temperature K	pressure Torr	flow rate cm s^{-1}	$[H_2O_2]$, 10^{13} molecule cm^{-3}	$[OH]_0$, 10^{11} molecule cm^{-3}	laser fluence mJ cm^{-2} $pulse^{-1}$	$[CHF_2CHFCHF_2]$, 10^{14} molecule cm^{-3}	k_3, 10^{-14} molecule cm^{-3} s^{-1}
238	51	6.2	2.47	1.79	4.1	9.53−46.5	0.80 ± 0.01[b]
238[a]	52	6.1	4.65	3.81	4.6	2.34−41.7	0.60 ± 0.01
254	52	6.6	2.74	2.37	4.8	4.38−41.8	1.03 ± 0.02
254[a]	52	6.6	9.40	7.27	4.3	3.07−43.9	0.79 ± 0.01
272	51	7.0	2.75	2.50	5.1	8.56−41.1	1.36 ± 0.04
272[a]	52	6.8	8.10	6.63	4.6	4.81−26.7	1.17 ± 0.06
297	63	6.2	2.59	2.94	6.4	8.39−65.6	2.02 ± 0.04
297	205	6.6	1.80	1.64	5.1	6.87−64.5	1.90 ± 0.04
297	55	7.5	8.35	7.60	5.1	9.58−52.1	1.93 ± 0.02
297	50	18.2	5.30	4.58	4.8	3.36−23.9	1.87 ± 0.06
324	51	8.2	3.56	3.08	4.8	3.56−27.8	2.68 ± 0.08
348	52	8.7	3.86	3.68	5.3	5.60−35.5	3.70 ± 0.08
374	50	9.50	6.05	5.23	4.8	3.73−28.9	4.75 ± 0.06

[a] Experiments carried out by passing the sample through a purification column containing sulfuric acid (20 wt %) deposited on Chromosorb WHP. [b] The quoted uncertainties are the 2σ (95% confidence limit) precision from the least-squares fit of the measured k' data to eq 6.

influence the determination of k_2. Kinetic measurements made using the purification method noted above also indicated that olefinic impurities were not a problem. The $CHF_2CHFCHF_2$ sample was contaminated with ~50 ppmv of $CF_3CH{=}CF_2$. To our knowledge, the rate coefficient for the reaction OH + $CF_3CH{=}CF_2$ has not been reported. However, using the rate coefficient[7] for the reaction of OH with $CH_3CH{=}CH_2$ (3×10^{-11} cm^3 $molecule^{-1}$ s^{-1}) and the measured abundance of this impurity, we compute the contribution of this unwanted reaction to be roughly 5% at 298 K increasing to 20% at 238 K. This analysis was verified when k_3 was measured using the purification method noted above. The k_3 value measured at the lowest temperature, 238 K, was lower by 20% compared with that measured using the sample without purification. Yet another possible indication of the reactive impurity was the slight curvature in the Arrhenius plot for k_3 shown in Figure 3. The influence of the impurity was also verified at 238, 254, and 272 K, and the results of these rate coefficient measurements are given in Table 3 and shown in Figure 3. The Arrhenius plot for k_3 measured using purified samples is almost linear. This analysis also shows (Figure 3) that the impurity contribution is negligible at 298 K and above. Therefore, the low temperature (<297 K) k_3 values obtained using the sample without purification were not used in the final Arrhenius fitting.

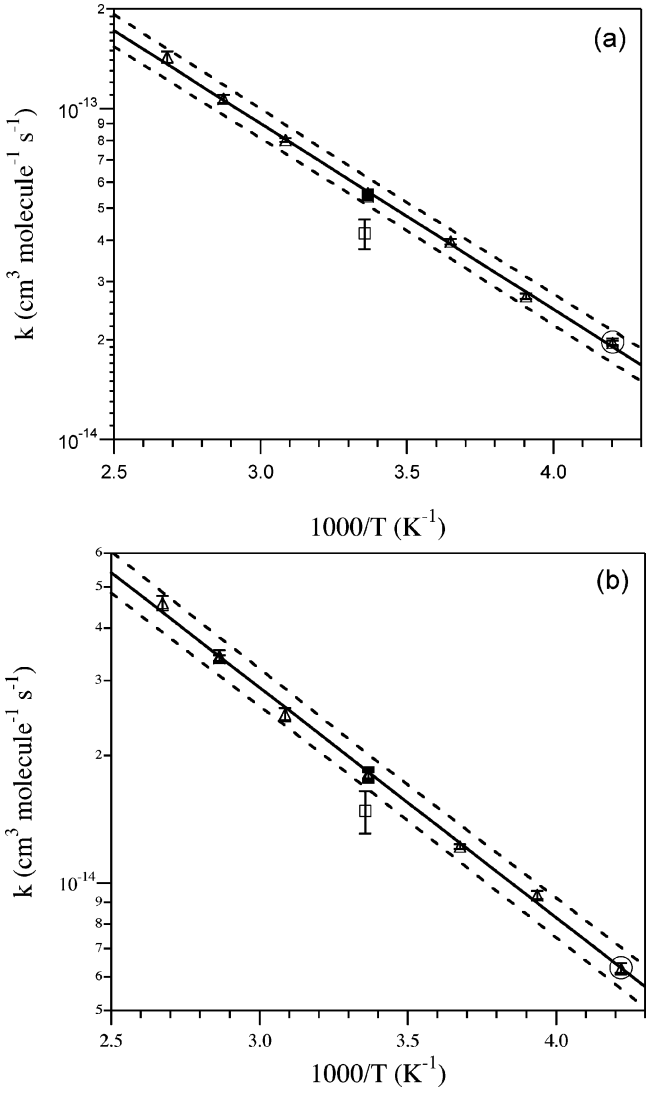

Figure 2. Arrhenius plot for the rate coefficient data obtained for the OH radical reaction with (a) $CF_3CH_2CH_3$ (k_1) and (b) CF_3CHFCH_2F (k_2) over the temperature range 238−373 K. The triangles correspond to data obtained with the unpurified sample and the circles to the data obtained with a purified sample. The solid lines are the linear least-squares fit to all the data (see text for details). The dashed lines represent the 2σ uncertainty limits, $f(T)$, calculated using $f(298\ \mathrm{K}) = 1.10$ and $g = 20$ (see text for definition of terms). The open squares are the room-temperature values reported by Nelson et al.[3]

The measured rate coefficients for the reaction of OH with $CF_3CH_2CH_3$, CF_3CHFCH_2F, and $CHF_2CHFCHF_2$ as a function of temperature are shown in Figures 2 and 3. As shown in Figure 2, the Arrhenius plots for reactions 1 and 2 are linear even when the unpurified samples of $CF_3CH_2CH_3$ and CF_3CHFCH_2F were used.

Other sources of systematic error in the rate coefficient determination include the possible influence of unwanted and unrecognized secondary reactions. The measured values of $k_{1-3}(T)$ were independent of the photolysis laser fluence, total pressure, flow velocity, and $[OH]_0$, as outlined in Tables 1−3. If the reactants absorbed the 248 nm photolysis radiation and generated free radicals that could react with OH, the measured rate coefficient would be dependent on photolysis laser fluence. The independence of the measured values of $k_{1-3}(T)$ with variations in laser fluence confirms that reaction of photolytic products with OH was not a problem.

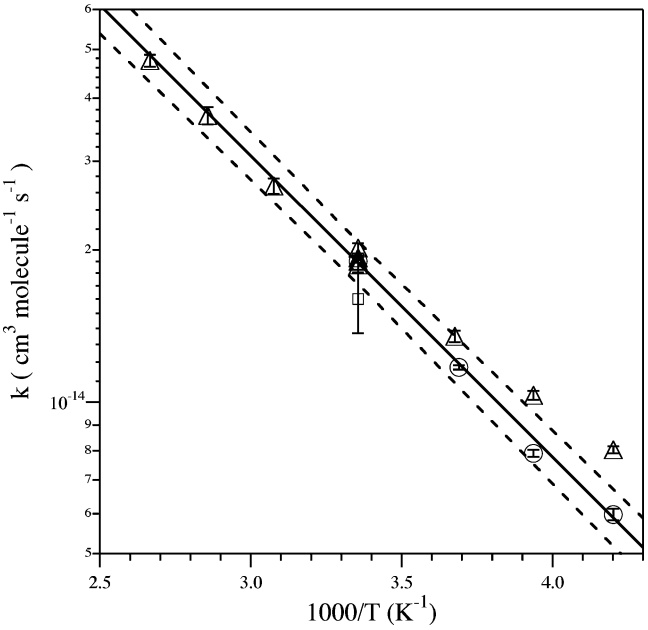

Figure 3. Arrhenius plot for the rate coefficient data obtained for the OH radical reaction with $CHF_2CHFCHF_2$ (k_3) over the temperature range 238−374 K. The triangles correspond to the data obtained with the unpurified sample and the circles to the data obtained with a purified sample. The solid line is the linear least-squares fit to the data obtained by using the purified samples (see text for details). The dashed lines represent the 2σ uncertainty limits, $f(T)$, calculated using $f(298\ \mathrm{K}) = 1.10$ and $g = 40$ (see text for definition of terms). The square corresponds to the room-temperature value reported by Nelson et al.[3]

An unweighted linear least-squares fit of the $k_{1-3}(T)$ data given in Tables 1, 2, and 3 to the equation, $\ln(k) = \ln(A) - (E/R)(1/T)$ yielded

$$k_1(T) = (4.36 \pm 0.63) \times 10^{-12} \exp[-(1293 \pm 42)/T]\ \mathrm{cm^3\ molecule^{-1}\ s^{-1}}$$

$$k_2(T) = (1.23 \pm 0.15) \times 10^{-12} \exp[-(1250 \pm 36)/T]\ \mathrm{cm^3\ molecule^{-1}\ s^{-1}}$$

$$k_3(T) = (1.91 \pm 0.39) \times 10^{-12} \exp[-(1377 \pm 60)/T]\ \mathrm{cm^3\ molecule^{-1}\ s^{-1}}$$

where the errors are 2σ from the precision of the fit and $\sigma_A = A\sigma_{\ln A}$. As discussed earlier, we estimate the uncertainty in the determination of the concentration of the reactant in the reactor to be 8% at the 95% confidence level. Propagation of this uncertainty into the above Arrhenius expressions and rounding off the uncertainties in E/R yields

$$k_1(T) = (4.36 \pm 0.72) \times 10^{-12} \exp[-(1290 \pm 40)/T]\ \mathrm{cm^3\ molecule^{-1}\ s^{-1}}$$

$$k_2(T) = (1.23 \pm 0.18) \times 10^{-12} \exp[-(1250 \pm 40)/T]\ \mathrm{cm^3\ molecule^{-1}\ s^{-1}}$$

$$k_3(T) = (1.91 \pm 0.42) \times 10^{-12} \exp[-(1375 \pm 100)/T]\ \mathrm{cm^3\ molecule^{-1}\ s^{-1}}$$

The possible impurity contribution to k_3, which decreases with increasing temperature, is assumed to contribute only to the E/R term. Hence, this uncertainty has been increased slightly. The

TABLE 4: Comparison of OH + $CF_3CH_2CH_3$, CF_3CHFCH_2F, and $CHF_2CHFCHF_2$ Rate Coefficients with Those from Previous Studies and Calculations

molecule	k(298 K)[a,b]	A[a]	$E/R \pm \Delta E/R$, K	T range, K	technique[c]	reference
$CF_3CH_2CH_3$ (HFC-263fb)	$(5.55 \pm 0.48) \times 10^{-14}$	$(4.36 \pm 0.72) \times 10^{-12}$	1290 ± 40	238−375	PLP-LIF	this work
	$(4.20 \pm 0.43) \times 10^{-14}$			298	DF-LIF	Nelson et al.[3]
	4.20×10^{-14}			298		JPL-2002[6]
	3.09×10^{-14}	3.16×10^{-12}	1385		IPC	Percival et al.[4]
	4.44×10^{-14}				SAR	Tokuhashi et al.[8]
CF_3CHFCH_2F (HFC-245eb)	$(1.81 \pm 0.18) \times 10^{-14}$	$(1.23 \pm 0.18) \times 10^{-12}$	1250 ± 40	238−375	PLP-LIF	this work
	$(1.48 \pm 0.17) \times 10^{-14}$			298	DP-LIF	Nelson et al.[3]
	1.50×10^{-14}			298		JPL-2002[6]
	7.41×10^{-15}	1.86×10^{-12}	1650		IPC	Percival et al.[4]
	1.05×10^{-14}				SAR	Tokuhashi et al.[8]
$CHF_2CHFCHF_2$ (HFC-245ea)	$(1.88 \pm 0.20) \times 10^{-14}$	$(1.91 \pm 0.42) \times 10^{-12}$	1375 ± 100	238−375	PLP-LIF	this work
	$(1.60 \pm 0.23) \times 10^{-14}$			298	DF-LIF	Nelson et al.[3]
	1.86×10^{-14}	2.63×10^{-12}	1475		IPC	Percival et al.[4]
	1.60×10^{-14}				SAR	Tokuhashi et al.[8]
$CF_3CF_2CH_3$ (HFC-245cb)	$(1.54 \pm 0.04) \times 10^{-15}$	$(4.41 \pm 0.80) \times 10^{-13}$	1690 ± 60	287−370	FP-RF	Orkin et al.[20]
$CF_3CH_2CF_3$ (HFC-236fa)	$(3.30 \pm 0.50) \times 10^{-16}$	$(1.45 \pm 0.22) \times 10^{-12}$	2500 ± 150	283−403	RR	Hsu and DeMore[21].

[a] Units of cm^3 $molecule^{-1}$ s^{-1}. [b] Quoted uncertainties from this work are at the 2σ level and include estimated systematic errors. Error limits from other studies are as quoted by the authors. [c] PLP: pulse laser photolysis. LIF: laser-induced fluorescence. DF: discharge flow. FP: flash photolysis. RF: resonance fluorescence. IPC: ionization potential correlation. RR: relative rate.

uncertainties in the format used in data evaluations[6] where the error at any given temperature, $f(T)$, is given by

$$f(T) = f(298\ \mathrm{K}) \exp\left|g\left(\frac{1}{T} - \frac{1}{298}\right)\right|$$

are $f(298\ \mathrm{K}) = 1.10$ and $g = 20$ for $CF_3CH_2CH_3$ and CF_3CHFCH_2F and $g = 40$ for $CHF_2CHFCHF_2$ but are given at the 2σ level. These uncertainty limits are shown in Figures 2 and 3.

The values of k_1, k_2, and k_3 obtained in this work are summarized in Table 4 along with those from the only other experimental determination by Nelson et al.[3] Nelson et al.[3] measured the rate coefficients $k_1 - k_3$ at room temperature using a discharge flow technique with laser-induced fluorescence detection of the OH radicals. The value of k_1(298 K) measured by Nelson et al.[3] is 4.20×10^{-14} cm^3 $molecule^{-1}$ s^{-1}, which is lower than our value by a factor of 1.3. The value of k_2(298 K) reported by Nelson et al.[3] is also lower than our value, by a factor of 1.2, but overlaps with ours within the combined uncertainty limits. The value of k_3(298 K) reported by the Nelson et al.[3] agrees with our value within the combined uncertainties. As discussed earlier, many variations of experimental parameters were used in our study to identify and minimize possible systematic errors. These tests give us added confidence in our results. The source of the small but measurable discrepancies with the rate coefficient data of Nelson et al.[3] is currently unknown.

We can also compare our measured rate coefficients with those obtained using structure activity relationships (SAR). Recently, Tokuhashi et al.[8] derived a set of SAR for fluorinated compounds using the methods previously developed in the works of Atkinson[9,10] and DeMore.[11] The rate coefficients calculated using the SAR analyses for $CF_3CH_2CH_3$, CF_3CHFCH_2F, and $CHF_2CHFCHF_2$ are included in Table 4. For $CF_3CH_2CH_3$ and $CHF_2CHFCHF_2$, the SAR rate coefficients are in good agreement (within 20%) with the experimental values. However, for CF_3CHFCH_2F, the SAR rate coefficient is lower than our experimental value by ~60%. The larger discrepancy is most likely due to the limited database available to derive the SAR factors for fluorinated compounds. Rate coefficient data for a series of OH + HFC reactions have also been reported by Percival et al.[4] Percival et al.[4] calculated Arrhenius parameters based on correlations with calculated ionization potentials of the HFCs. The results for the molecules studied in this work are given in Table 4 and are found to be in reasonable agreement with the experimental values.

The activation energy, E, for these reactions depends on the number and reactivities of reaction sites available and the number of F atoms present in the molecule. Out of the three molecules we have studied, the OH + $CF_3CH_2CH_3$ reaction is expected to have a lower E than the other two molecules, as it has two F free sites, more H atoms, and two secondary hydrogens. We have used the SAR method [8](derived by Tokuhashi et al.) to evaluate the contribution of each site in the molecule toward the rate coefficient. In $CF_3CH_2CH_3$, the contribution of the CH_2 group is calculated to be only 7%, while the rest of the reaction is due to the CH_3 group. This is a surprisingly small contribution. The SAR calculations using DeMore's group contributions[11] indicate that both CH_2 and CH_3 groups contribute almost equally to the overall reaction. This conclusion appears to be more reasonable. We attribute the low value of the calculated contribution by the CH_2 group using the Tokuhashi et al.'s group factors to an error in their group contributions, which were derived to optimize the predictability for a different set of functional groups. However, it should be noted that the calculated overall rate coefficient is reasonably close to the measured value.

When CH_2 is replaced with CF_2 in $CF_3CF_2CH_3$, the reaction must be exclusively due to H-atom abstraction from the CH_3 group; accordingly, there should be an increase in the activation energy as is observed (see Table 4). However, when the CH_3 group is replaced with CF_3 in $CF_3CH_2CF_3$, the E/R is raised further by ~1000 K, which is again reasonable, because the reaction is solely due to the CH_2 group which is influenced by two CF_3 groups. In the case of CF_3CHFCH_2F, the contribution of both CHF and CH_2F groups is evaluated to be ~50% of the total reaction, using the methods of both Tokuhashi et al.[8] and DeMore.[11] In $CHF_2CHFCHF_2$, using Tokuhashi's[8] method, each

CHF_2 group was found to contribute 25% and the CHF group contributed 50% to the total reaction. DeMore's[11] method suggests the contributions of each CH_2F group to be 32% and that of the CHF group to be 36%. The *E*/*R* for these two molecules turn out to be similar. Therefore, the atmospheric degradation of CF_3CHFCH_2F and $CHF_2CHFCHF_2$ will proceed via multiple pathways with different possible end products.

Atmospheric Implications

Lifetimes. The atmospheric lifetime of any compound that is released into the atmosphere depends on the rates of all processes that remove it. It may be lost by photolysis, wet and dry deposition, rain out, and reaction with free radicals (especially OH radicals). The UV absorption cross-sections of the HFCs included in the current investigation, at wavelengths greater than 300 nm, are expected to be very small. Therefore, photolytic loss of these compounds is negligible. Because of the presence of C−H bonds in HFCs, they are lost in the atmosphere mostly via their reactions with OH radicals. Atmospheric lifetimes for gases destroyed primarily by reaction with OH can be best evaluated using constraints on global OH densities derived from methyl chloroform measurements.[12,13] The analysis of Prinn et al.,[12] using measured global methyl chloroform abundance during the past 25 years, together with detailed information on production, release, and transport of this solely industrial gas provides the most complete assessment of the globally averaged OH density. We use the OH values and the general approach given by Prinn et al.[12] to derive OH-driven lifetimes for $CF_3CH_2CH_3$, CF_3CHFCH_2F, and $CHF_2CHFCHF_2$ using a two-box (stratosphere and troposphere) assumption. With this method, the OH-driven lifetimes of $CF_3CH_2CH_3$, CF_3CHFCH_2F, and $CHF_2CHFCHF_2$ were estimated to be 0.8, 2.6, and 2.5 years, respectively.

Global Warming Potentials. Global warming potentials (GWP) are a measure of the time-integrated radiative forcing of the climate system due to a pulse release of a particular gas, relative to a reference molecule (usually taken to be carbon dioxide).[14,15] As such, they can be very useful in evaluating the relative climatic implications of the use of one halocarbon substitute compared to another. To compute the GWP, one needs the radiative forcing, the lifetime of the gas, and the time-integrated radiative forcing of the reference gas (we use those given for CO_2 in WMO-2003[1]). We compute the adjusted all-sky radiative forcing using a line-by-line (LBL) radiative transfer model developed by Portmann et al.[16] (see also Forster et al.[17]). The infrared absorption cross-sections of $CF_3CH_2CH_3$, $CF_3CHFCHF_2$, and $CHF_2CHFCHF_2$ measured in this work and shown in Figure 4 were used. Pinnock et al.[18] have presented a detailed analysis of the sensitivity of GWPs to other factors, such as band overlaps with gases such as H_2O, CO_2, and so forth, global averaging potentials, and background atmospheres. We have accurately included all of these effects, with the exception of the stratospheric falloff of the molecule (which could reduce these estimates by up to 10%). The line-by-line code used here numerically integrates the radiative transfer equation to evaluate the upward, downward, and net irradiance at each level in the atmosphere. We employ the ISCCP monthly mean zonally averaged profiles of pressure, temperature, H_2O, CO_2, and O_3, and fields of CH_4 and N_2O derived from the NOCAR model. The absorption spectra for these gases have been taken from the HITRAN-2000 database.[19] Spectral overlap between these gases and $CF_3CH_2CH_3$, $CF_3CHFCHF_2$, and $CHF_2CHFCHF_2$ are considered. The globally and annually averaged radiative forcing for $CF_3CH_2CH_3$, $CF_3CHFCHF_2$, and $CHF_2CHFCHF_2$ were found to be 0.13, 0.23, and 0.18 W m^{-2} $ppbv^{-1}$, respectively. For comparison, the radiative forcing by CFC-11 is 0.25 W m^{-2} $ppbv^{-1}$.[1]

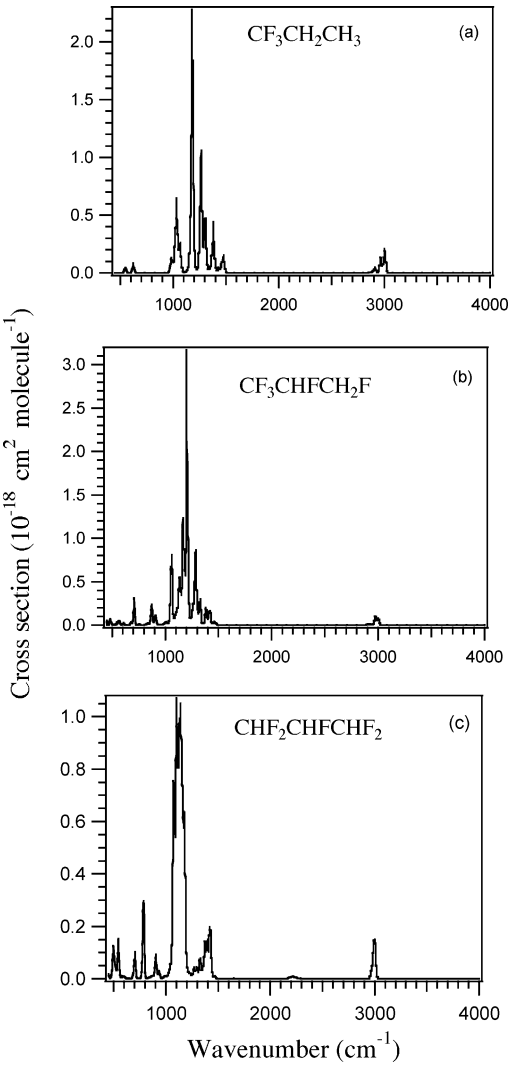

Figure 4. Infrared absorption spectra of (a) $CF_3CH_2CH_3$, (b) CF_3CHFCH_2F, and (c) $CHF_2CHFCHF_2$ in the region 500−4000 cm^{-1} recorded at 1 cm^{-1} resolution measured using pure samples, i.e., with no bath gas added.

TABLE 5: Global Warming Potential (GWP) (mass basis) Referenced to the Decay Response for CO_2

molecule	lifetime (years)	radiative forcing (W m^{-2} $ppbv^{-1}$)	global warming potential time horizons (years) 20	100	500
$CF_3CH_2CH_3$ (HFC-263fb)	0.8	0.13	234	69.6	21.7
CF_3CHFCH_2F (HFC-245eb)	2.6	0.23	962	286	89.2
$CHF_2CHFCHF_2$ (HFC-245ea)	2.5	0.18	723	215	67.8

Table 5 presents the GWPs for $CF_3CH_2CH_3$, $CF_3CHFCHF_2$, and $CHF_2CHFCHF_2$ for the same time periods given in WMO-2003[1] (to which they can be directly compared, since the same time-integrated radiative forcing of CO_2 has been used). The information in this table provides a basis for evaluating the relative climatic impacts of choices between a large number of short- and long-lived halocarbon substituents.

To conclude, though the atmospheric lifetimes of $CF_3CH_2CH_3$, $CF_3CHFCHF_2$, and $CHF_2CHFCHF_2$ are reasonably long, they may be considered short-lived when compared

to CFCs. Their GWPs are also relatively smaller than those of CFCs (e.g., CFC-11 with a GWP of 6330 for 20-year time horizon) primarily because of their shorter lifetimes. They do not contribute to stratospheric ozone depletion. Hence, these compounds may be suggested as acceptable substitutes to CFCs.

Acknowledgment. We thank Stephen Montzka for the help in analyzing the HFC samples by GCMS. We thank David Nelson and Charles Kolb of Aerodyne research for providing the samples used in this study. This work was funded in part by NOAA's climate program. A.R.R. thanks Dave Golden for his friendship, encouragement, and scientific interchanges over the past three decades.

References and Notes

(1) *WMO Scientific Assessment of Ozone Depletion 2002*; Global Ozone research monitoring project no. 47, Geneva, 2003.

(2) *Montreal Protocol on Substances that Deplete the Ozone Layer*; United Nations Environmental Program (UNEP), Geneva, Switzerland, 1987.

(3) Nelson, D. D.; Zahniser, M. S.; Kolb, C. E.; Magid, H. *J. Phys. Chem. A* **1995**, *99*, 16301.

(4) Percival, C. J.; Marston, G.; Wayne, R. P. *Atmos. Environ.* **1995**, *29*, 305.

(5) Vaghjiani, G. L.; Ravishankara, A. R. *J. Phys. Chem.* **1989**, *93*, 1948.

(6) Sander, S. P.; Friedl, R. R.; Golden, D. M.; Huie, R. E.; Kolb, C. E.; Kurylo, M. J.; Molina, M. J.; Moortgat, G. K.; Orkin, V. L.; Ravishankara, A. R.; Finlayson-Pitts, B. J. *Chemical kinetics and photochemical data for use in atmospheric studies*; JPL Publication 02−25; Jet Propulsion Laboratory: Pasadena, 2002; Evaluation Number 14.

(7) Nielsen, O. J.; Jorgensen, O.; Donlon, M.; Sidebottom, H. W.; O'Farrell, D. J.; Treacy, J. *Chem. Phys. Lett.* **1990**, *168*, 319.

(8) Tokuhashi, K.; Nagai, H.; Takahashi, A.; Kaise, M.; Kondo, S.; Sekiya, A.; Takahashi, M.; Gotoh, Y.; Suga, A. *J. Phys. Chem. A* **1999**, *103*, 2664.

(9) Atkinson, R. *Int. J. Chem. Kinet.* **1987**, *19*, 799.

(10) Kwok, E. S. C.; Atkinson, R. *Atmos. Environ.* **1995**, *29*, 1685.

(11) DeMore, W. B. *J. Phys. Chem.* **1996**, *100*, 5813.

(12) Prinn, R.; Weiss, R.; Millar, B.; Jaung, J.; Alyea, F.; Cunnold, D.; Fraser, P.; Hartley, D.; Simmonds, P. *Science* **1995**, *269*, 187.

(13) Prinn, R.; Cunnold, D.; Simmonds, P.; Alyea, F.; Boldi, R.; Crawford, A.; Fraser, P.; Gutzler, D.; Hartley, D.; Rosen, R.; Rasmussen, R. *J. Geophys. Res., [Atmos.]* **1992**, *97*, 2445.

(14) *Radiative forcing of climate change and an evaluation of the IPCC IS92 Emission Scenarios*; Houghton, J. T., Filho, L. G. M., Bruce, B., Lee, H., Callander, B. A., Haites, E., Harris, N., Maskell, K., Eds.; Intergovernmental Panel on Climate Change (IPCC), climate change, 1994; Cambridge University Press: New York, 1995.

(15) *Climate Change, The IPCC Scientific assessment*; Houghton, J. T., Jenkins, G. J., Ephraums, J. J., Eds.; Cambridge University Press: New York, 1990.

(16) Portmann, R. W.; Solomon, S.; Fishman, J.; Olson, J. R.; Kiehl, J. T.; Briegleb, B. *J. Geophys. Res., [Atmos.]* **1997**, *102*, 9409.

(17) Forster, P. M. D.; Burkholder, J. B.; Clerbaux, C.; Coheur, P. F.; Dutta, M.; Gohar, L. K.; Hurley, M. D.; Myhre, G.; Portmann, R. W.; Shine, K. P.; Wallington, T. J.; Wuebbles, D. *J. Quant. Spectrosc. Radiat. Transfer* **2005**, *93*, 447.

(18) Pinnock, S.; Hurley, M. D.; Shine, K. P.; Wallington, T. J.; Smyth, T. J. *J. Geophys. Res., [Atmos.]* **1995**, *100*, 23227.

(19) Rothman, L. S.; Barbe, A.; Benner, D. C.; Brown, L. R.; Camy-Peyret, C.; Carleer, M. R.; Chance, K.; Clerbaux, C.; Dana, V.; Devi, V. M.; Fayt, A.; Flaud, J. M.; Gamache, R. R.; Goldman, A.; Jacquemart, D.; Jucks, K. W.; Lafferty, W. J.; Mandin, J. Y.; Massie, S. T.; Nemtchinov, V.; Newnham, D. A.; Perrin, A.; Rinsland, C. P.; Schroeder, J.; Smith, K. M.; Smith, M. A. H.; Tang, K.; Toth, R. A.; Vander Auwera, J.; Varanasi, P.; Yoshino, K. *J. Quant. Spectrosc. Radiat. Transfer* **2003**, *82*, 5.

(20) Orkin, V. L.; Huie, R. E.; Kurylo, M. J. *J. Phys. Chem. A* **1997**, *101*, 9118.

(21) Hsu, K. J.; DeMore, W. B. *J. Phys. Chem.* **1995**, *99*, 1235.